

Supporting Information for

Highly Open Chalcogenide Frameworks Built from Unusual Defective Supertetrahedral Cluster

Chaozhuang Xue, Li Zhang, Xiaoli Wang, Xiang Wang, Jiaxu Zhang and Tao Wu*

College of Chemistry, Chemical Engineering and Materials Science, Soochow University, Suzhou,
Jiangsu 215123, China.

Experimental Section:

Chemicals and Materials. Indium powder (In, 99.99%), selenium powder (Se, $\geq 99.5\%$), 3, 5-dimethylpiperidine ($C_7H_{15}N$, $\geq 99\%$), 3-methylpiperidine ($C_6H_{13}N$, $\geq 99.5\%$), amino trimethylene phosphonic acid (ATMP, 50%, liquid) and deionized water all used without any further purification.

Synthesis of CSZ-11: The mixture of indium (80 mg), selenium (250 mg), 3, 5-dimethylpiperidine (2.5 mL), deionized water (1 mL) and amino trimethylene phosphonic acid (1 mL) were added into a 23 mL Teflon-lined stainless steel autoclave, and stirred for 2 h at room temperature. The vessel was then sealed and heated at 170 °C for 5 days. The autoclave was subsequently allowed to cool to room temperature. 20 mg of saffron-yellow prismatic crystals were obtained.

Synthesis of CSZ-12: The mixture of indium (80 mg), selenium (250 mg), 3-methylpiperidine (2.5 mL) and deionized water (1 mL) were added into a 23 mL Teflon-lined stainless steel autoclave, and stirred for 2 h at room temperature. The vessel was then sealed and heated at 170 °C for 5 days. The autoclave was subsequently allowed to cool to room temperature. 80 mg of saffron-yellow prismatic crystals were obtained.

Structure Characterization. The single-crystal X-ray diffraction measurements was performed on a Bruker Smart CPAD area diffractometer with nitrogen-flow temperature controller using graphite-monochromated $MoK\alpha$ ($\lambda = 0.71073 \text{ \AA}$) radiation at 120 K. The absorption correction on CSZ-11 and CSZ-12 were performed using program of 'multi-scan' in APEX 3 with the input parameters including Mean $I/\sigma(I)$ Threshold : 1.5, high resolution threshold: 0.1, factor g for initial weighting scheme: 0.04, Restraint EDS for scale factors: 0.005, absorption type: medium absorber, number of refinement cycles: 50, marquardt damping factor: 0.0001. The structure was solved by direct method using SHELXS-2014 and the refinement against all reflections of the compounds was performed using SHELXL-2014. Solvent molecules were removed from the data set using the SQUEEZE routine of PLATON and refined further using the data generated. Powder X-ray diffraction (PXRD) data were collected on a desktop diffractometer (D2 PHASER, Bruker, Germany) using $Cu-K\alpha$ ($\lambda=1.54056 \text{ \AA}$) radiation operated at 30 kV and 10 mA.

Elemental Analysis. Energy dispersive spectroscopy (EDS) analysis was performed on scanning electron microscope (SEM) equipped with energy dispersive spectroscopy (EDS) detector. An accelerating voltage of 25 kV and 40 s accumulation time were applied.

Thermogravimetric (TG) Measurement. A Shimadzu TGA-50 thermal analyzer was used to

measure the TG curve by heating the sample from room temperature to 800 °C with heating rate of 10 °C/min under N₂ flow.

Optical Measurements: Room-temperature solid-state UV-vis diffusion reflectance spectra of crystal samples were measured on a SHIMADZU UV-3600 UV-Vis-NIR spectrophotometer, by using BaSO₄ powder as the reflectance reference. The absorption spectra were calculated from reflectance spectra by using the Kubelka-Munk function: $F(R)=\alpha/S=(1-R)^2/2R$, where R , α , and S are the reflection, the absorption and the scattering coefficient, respectively. In order to determine band edge of the direct gap semiconductor, the relation between the absorption coefficients (α) and the incident photon energy ($h\nu$) is exhibited as $\alpha h\nu = A(h\nu - E_g)^{1/2}$, where A is a constant that relates to the effective masses associated with the valence and conduction bands, and E_g is the optical transition gap of the solid material. The band gap of the obtained samples can be determined from the Tauc plot with $[F(R)*h\nu]^2$ vs. $h\nu$ by extrapolating the linear region to the abscissa.

Ion-Exchange Experiments. Typically, 10 mg of as-synthesized sample was added into 10 mL of aqueous solution of standard Cs⁺ solution (1 M). The mixture was kept shaking for 15–18 h at room temperature. And then the sample with darker color were isolated by filtration and washed by water and ethanol for several times.

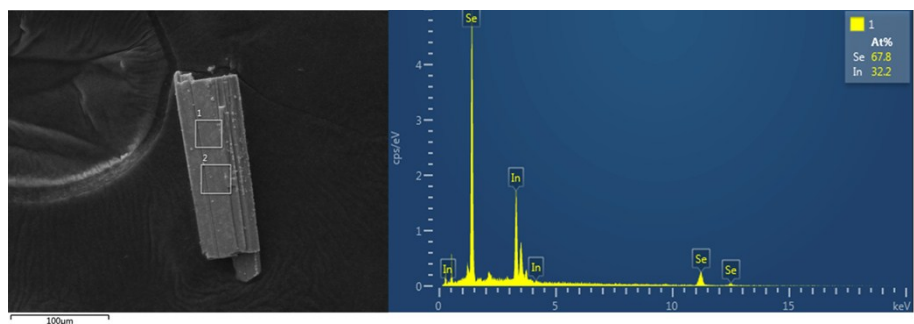


Fig. S1 SEM image (left) and energy (right) dispersive spectroscopy (EDS) of CSZ-11.

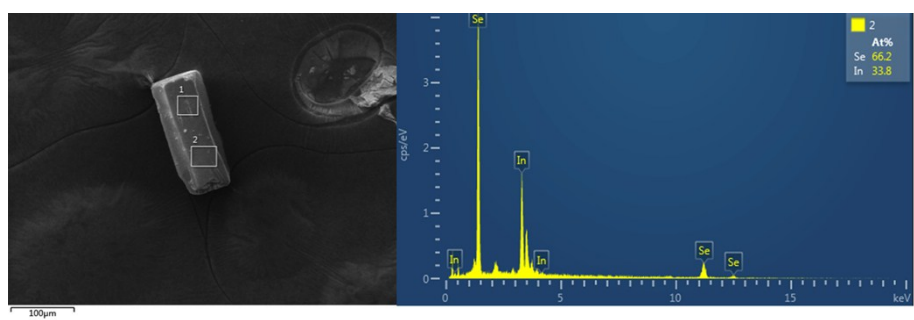


Fig. S2 SEM image (left) and energy (right) dispersive spectroscopy (EDS) of CSZ-12.

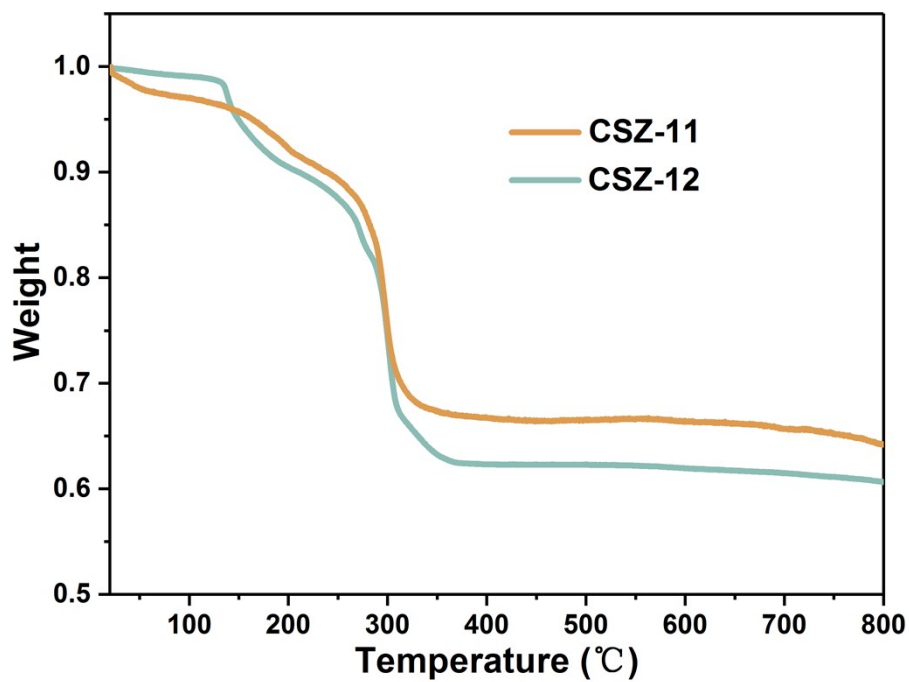


Fig. S3 TGA curves of CSZ-11 and CSZ-12.

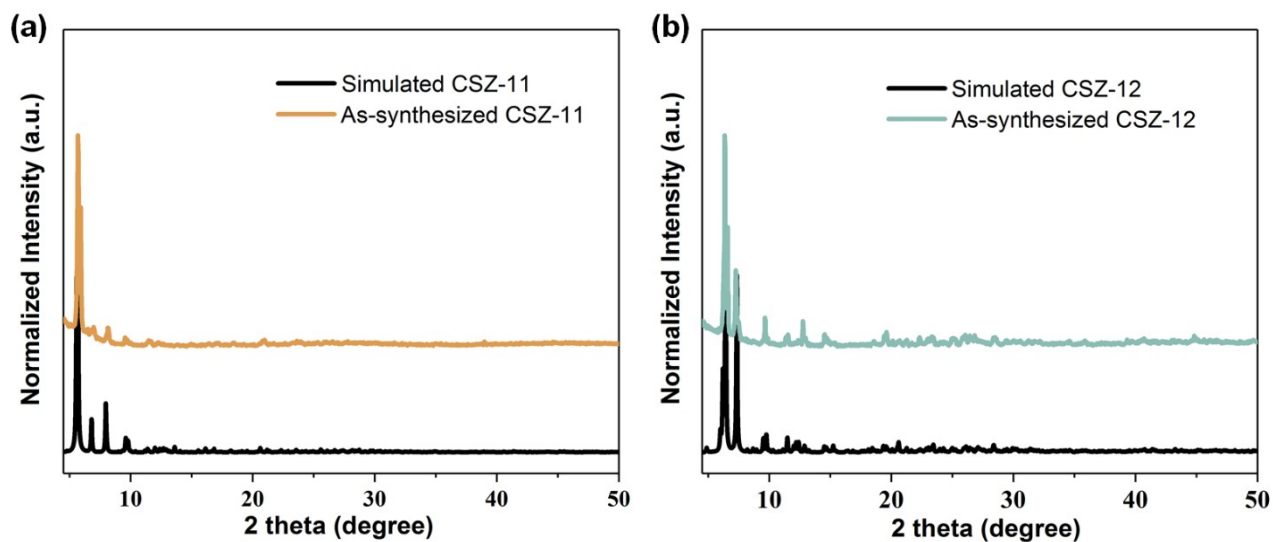


Fig. S4 Powder X-ray diffraction (PXRD) patterns of the simulated structure models and as-synthesized samples of CSZ-11 (a) and CSZ-12 (b).

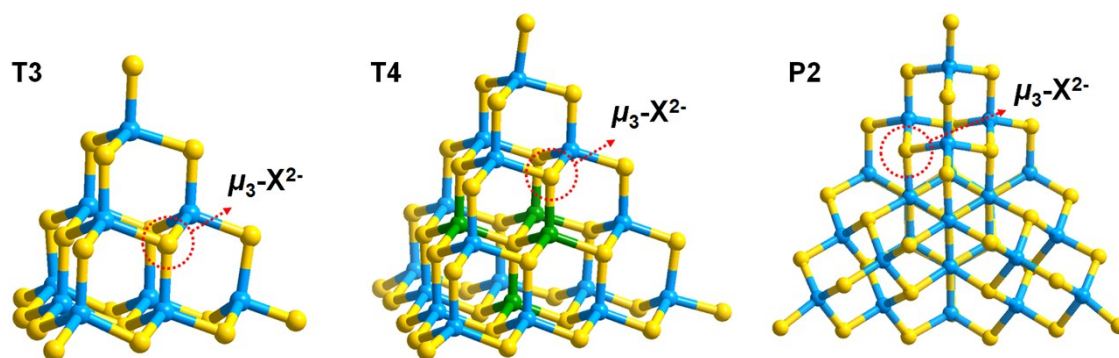


Fig. S5 T3, T4 and P2 clusters (red dotted-line: $\mu_3\text{-X}^{2-}$, X = S/Se).

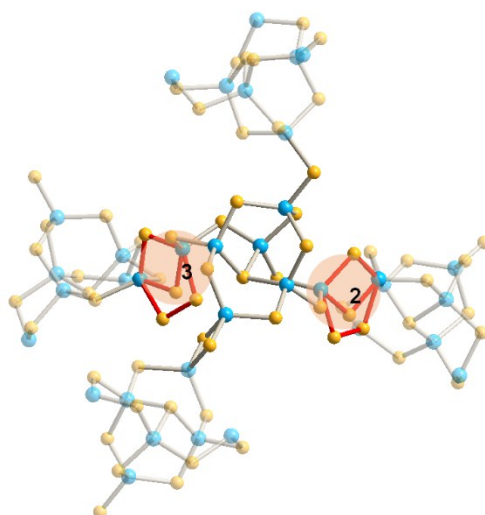


Fig. S6 Five-membered ring of In_2Se_3 and four-membered ring of In_2Se_2 are position-shared at site 2 and 3 in CSZ-11.

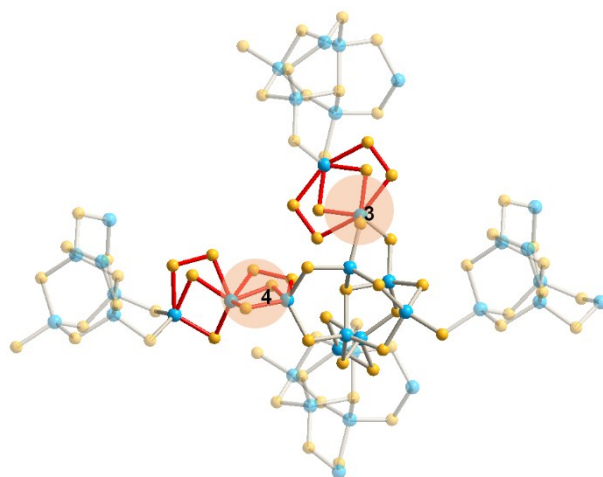


Fig. S7 Disorder linkers at site 3 and 4 in CSZ-12.

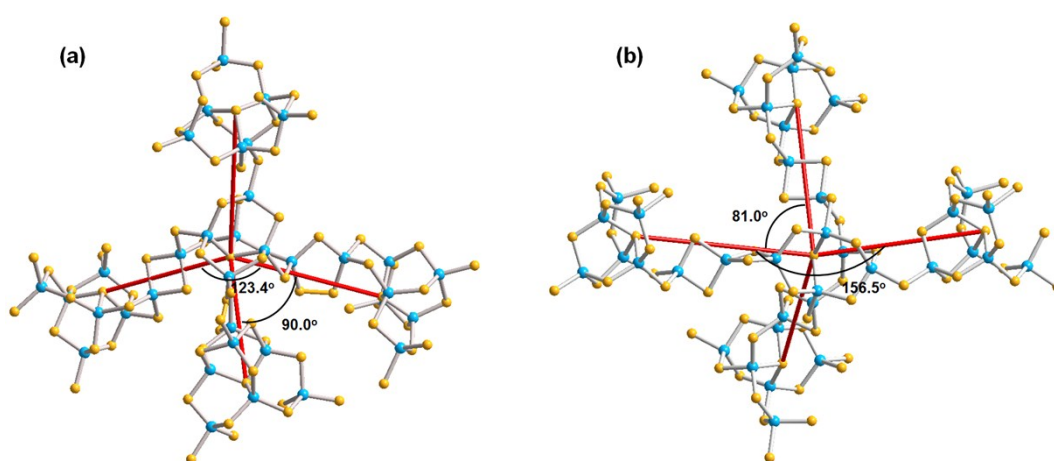


Fig. S8 The maximum angle and minimum angle of the adjacent three clusters in CSZ-11 (a) and CSZ-12 (b).

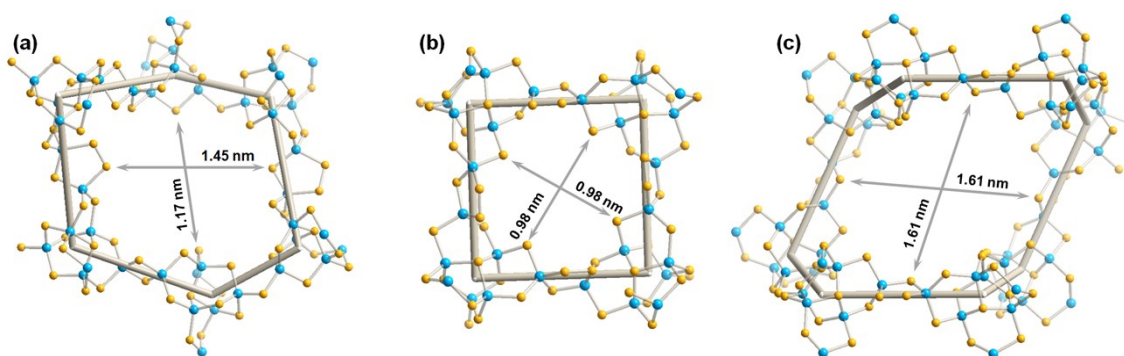


Fig. S9 Three kinds of window in CSZ-11. (a) Six-membered ring of window A (viewed from a/b -axis). (b) Four-membered ring of window B (viewed from c -axis). (c) Eight-membered ring of window C (viewed from c -axis).

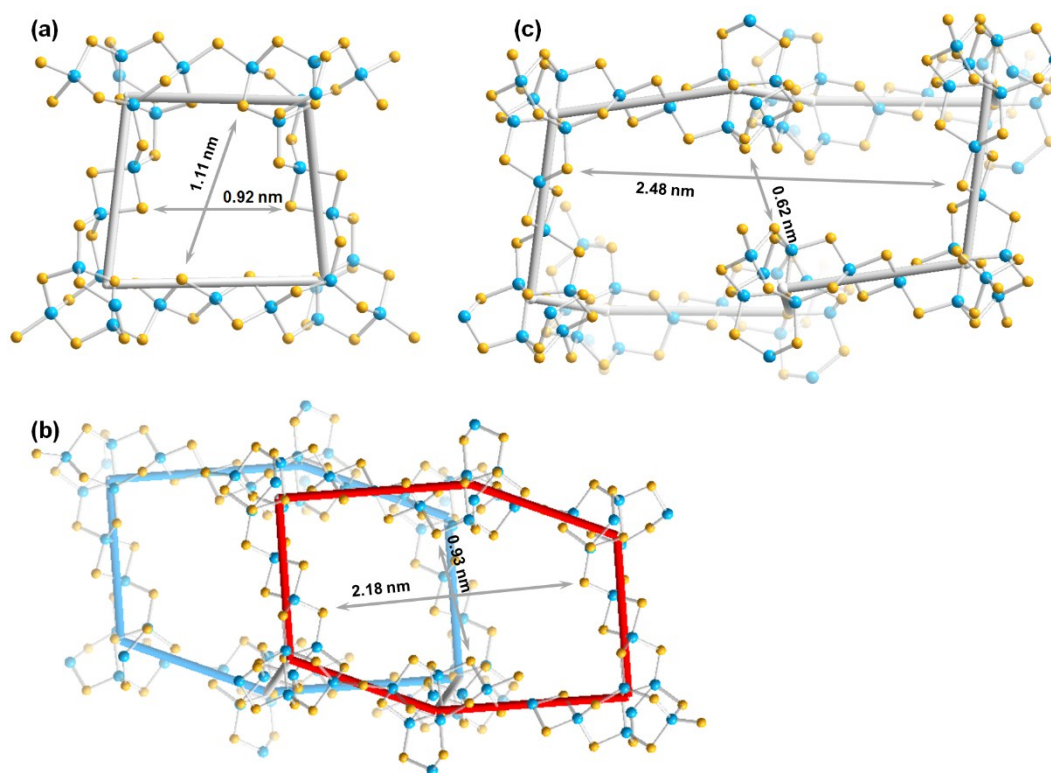


Fig. S10 Three kinds of windows in CSZ-12. (a) Four-membered ring of window D (viewed from a -axis). (b) Interlaced six-membered ring of window E (viewed from b -axis). (c) Ten-membered ring of window F (viewed from c -axis).

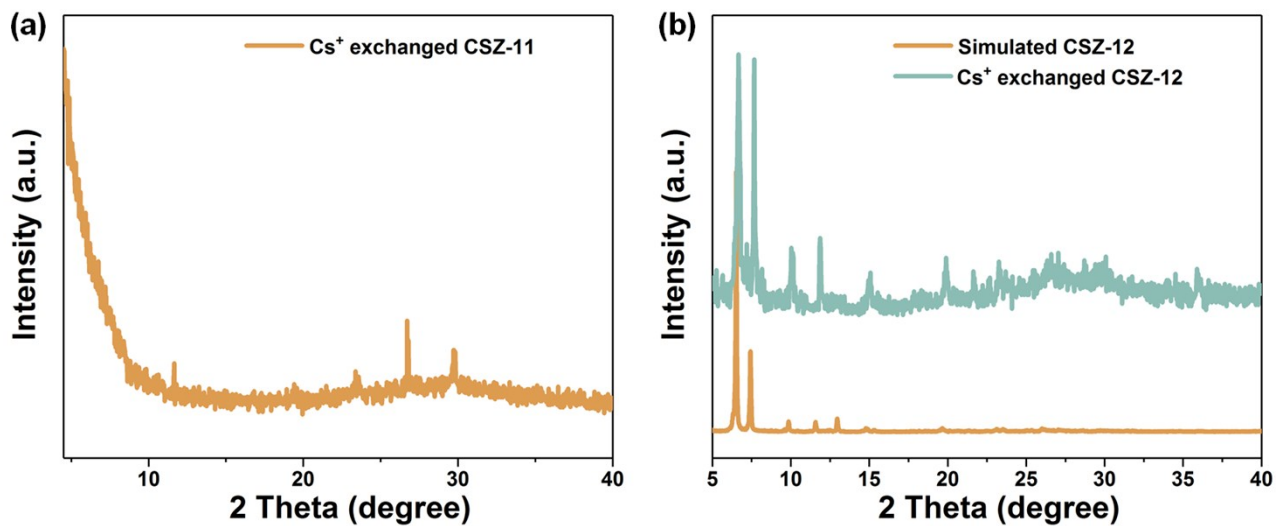


Fig. S11 PXR D patterns of Cs⁺ exchanged CSZ-11 (a) and CSZ-12 (b).

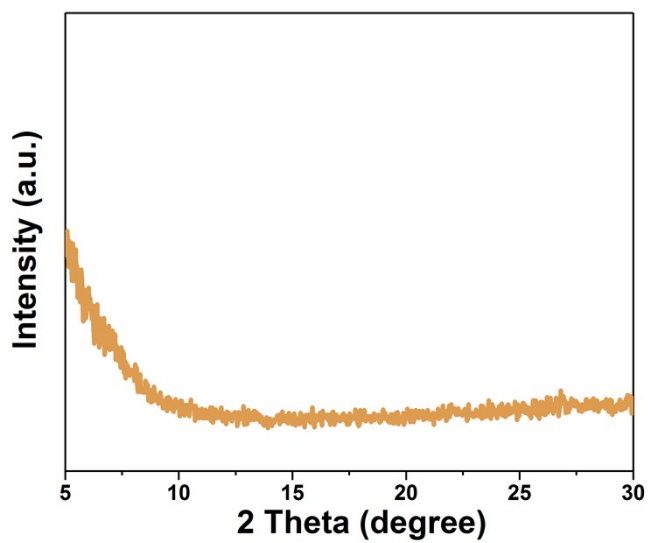


Fig.S12 PXR D pattern of CSZ-12 after degassing process.

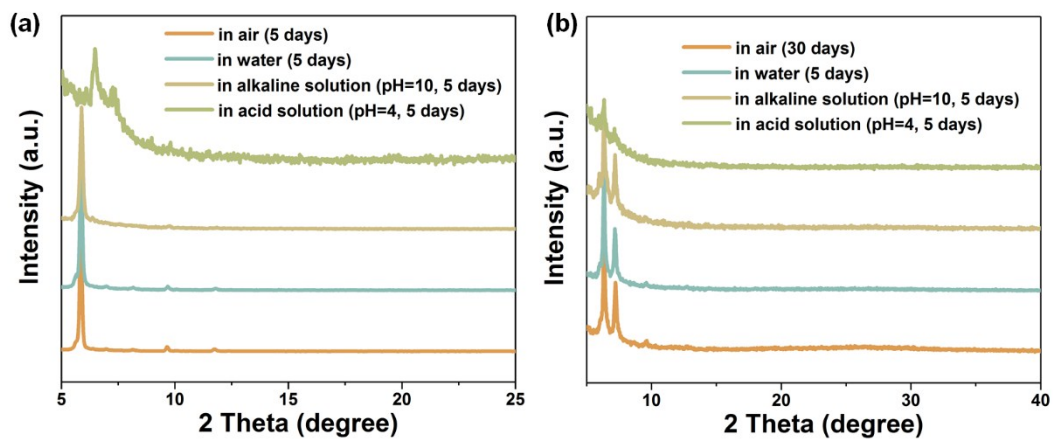


Fig. S13 The powder X-ray diffraction patterns for **CSZ-11** (a) and **CSZ-12** (b) after exposed in different conditions with several days.

Table S1. Crystal data and structure refinement parameters for **CSZ-11** and **CSZ-12**.

Compounds	CSZ-11	CSZ-12
Crystal system	tetragonal	monoclinic
Space group	<i>P4/ncc</i>	<i>C2/c</i>
<i>Z</i>	1	1
<i>a</i> (Å)	31.0100 (17)	27.6136 (10)
<i>b</i> (Å)	31.0100 (17)	24.8147 (10)
<i>c</i> (Å)	36.8077 (14)	24.0930 (9)
α (deg.)	90	90
β (deg.)	90	93.6160
γ (deg.)	90	90
<i>V</i> (Å ³)	35395 (4)	16476.2(10)
GOF on <i>F</i> ²	1.028	1.147
<i>R</i> ₁ , <i>wR</i> ₂ (<i>I</i> > 2σ(<i>I</i>))	0.066, 0.1835	0.0519, 0.1704
<i>R</i> ₁ , <i>wR</i> ₂ (all data)	0.1083, 0.2165	0.0873, 0.1960

Table S2. Elemental analysis results of **CSZ-11** and **CSZ-12**.

Elements (wt.)	N (%)	C (%)	H (%)
Calculated for CSZ-11	3.9	23.5	4.5
Experimental for CSZ-11	3.7	24.0	4.6
Calculated for CSZ-12	3.4	17.7	3.2
Experimental for CSZ-12	3.5	16.0	3.3